Gem News International

Contributing Editors
Emmanuel Fritsch, *University of Nantes, CNRS, Team 6502, Institut des Matériaux Jean Rouxel (IMN), Nantes, France* (fritsch@cnrs-imn.fr)
Gagan Choudhary, *Gem Testing Laboratory, Jaipur, India* (gagan@gjepcindia.com)
Christopher M. Breeding, *GIA, Carlsbad* (christopher.breeding@gia.edu)

COLORED STONES AND ORGANIC MATERIALS

Blue gahnite from Nigeria. In recent years, Nigeria has gained considerable attention in the gem trade for the discovery of sapphires reportedly from the Mambilla Plateau in Taraba State. In addition to sapphires, spinels have been sporadically mined in Jemaa and recently in Kagoro, both in Kaduna State (figure 1). The spinel group of minerals, with a general chemical formula AB_2O_4, has a total of 22 different species. Four of these species have Al predominantly occupying the octahedral site: spinel ($MgAl_2O_4$), galaxite ($MnAl_2O_4$), hercynite ($FeAl_2O_4$), and gahnite ($ZnAl_2O_4$). The spinels from Kagoro have been identified as gahnite, the zinc end member. Gahnite is one of the rarer members of the spinel group of minerals, typically found at zinc deposits. Most crystals are very small, included, and translucent to opaque. Faceted gems are very collectible due to their rarity and color.

The geology of the Nigerian spinels has been previously studied (R. Jacobson and J.S. Webb, "The pegmatites of central Nigeria," *Geological Survey of Nigeria Bulletin*, No. 17, 1946, pp. 1–61), and the deposits can be subdivided into three groups based on their mineralogy: (1) microcline-quartz pegmatites, which commonly occur within the calc-alkaline granitoids and are rarely mineralized; (2) microcline-quartz-mica pegmatites, found within metasedimentary sequences; and (3) quartz-mica veins, which occur in schists and gneisses or marginal to group 2 pegmatites. Gahnite occurs in groups 2 and 3. Knowledge of the composition of zinc-rich spinels is useful in separating a wide variety of source environments. For example, Zn content is high in spinels occurring in rocks that have experienced low-grade metamorphism and high oxygen and sulfur fugacity (fO_2 and fS_2), whereas Zn content is lowest in high-grade metamorphic rocks (A. Heimann et al., "Zincian spinel associated with metamorphosed Proterozoic base-metal sulfide occurrences, Colorado: A re-evaluation of gahnite composition as a guide in exploration," *Canadian Mineralogist*, Vol. 43, No. 2, 2005, pp. 601–622).

Figure 1. Three single octahedra of natural gahnite, approximately 1.5 ct each, from Kaduna State, Nigeria. Photo by Robison McMurtry.

Standard gemological examination of three rough octahedra (figure 1) gave the following properties: color—blue; pleochroism—none; refractive index—1.791 to over the limit (flat reading from polished crystal face); hydrostatic specific gravity—4.180–4.294; fluorescence reaction—inert to both long- and short-wave UV; and color filter reaction—red. Internal characteristics observed with a gemological microscope were colorless unidentified crystals, fingerprints, and a red-brown crystal inclusion identified by Raman spectroscopy as sphalerite (figure 2).

Editors' note: Interested contributors should send information and illustrations to Stuart Overlin at soverlin@gia.edu or GIA, The Robert Mouawad Campus, 5345 Armada Drive, Carlsbad, CA 92008.

Gems & Gemology, Vol. 55, No. 3, pp. 434–455.

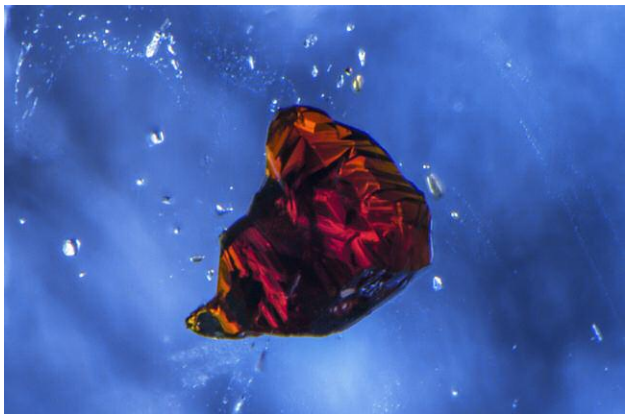

Figure 2. Raman identification of this inclusion was consistent with sphalerite. Photomicrograph by Nathan Renfro; field of view 0.91 mm.

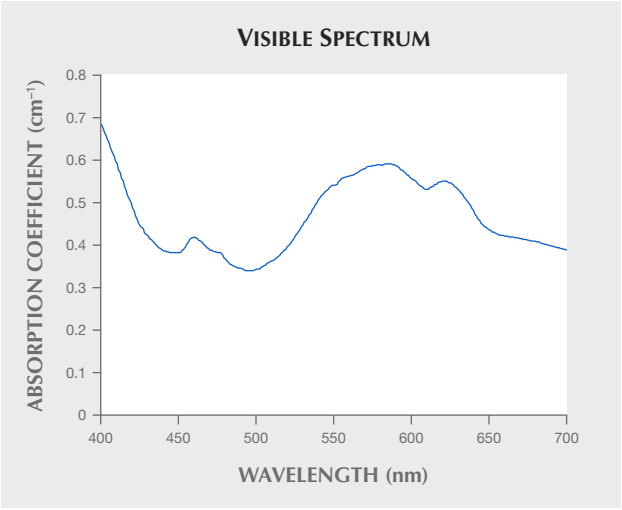

Figure 3. The visible spectrum of the Nigerian gahnite from Kagoro. The absorption bands from ~500 to 650 nm are largely due to Co^{2+}, but with modification from iron absorption bands. Absorption bands around 462 and 470 nm are related to iron chromophores.

Advanced spectroscopic testing was performed on the three samples. The Raman spectra were typical of gahnite, with peaks at 420, 510, and 661 nm. The visible spectrum showed significant cobalt absorption bands (figure 3) between 500 and 620 nm, with additional contribution from iron absorption bands modifying the cobalt absorption spectrum (e.g., A.C. Palke and Z. Sun, "What is cobalt spinel? Unraveling the causes of color in blue spinels," Fall 2018 *G&G*, pp. 262–263).

Figure 4. A vertical line 1 and a horizontal line 2, containing a total of 44 spots, were selected to apply LA-ICP-MS analyses across the whole section. Mol.% end member vs. position profiles revealed that the stone was predominantly composed of gahnite with minor hercynite, spinel, and galaxite. Detailed information on major element chemistry, site distribution, and species for each spot can be found in appendix 1 online. Spot spacing is 200 microns.

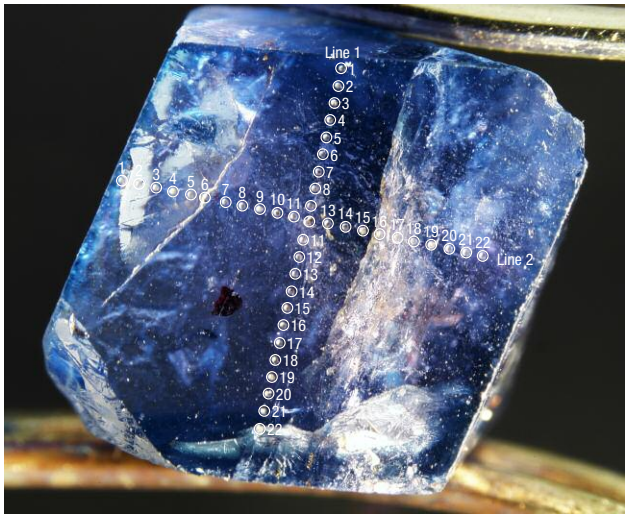

Laser ablation–inductively coupled plasma–mass spectrometry (LA-ICP-MS) analysis was used to obtain the accurate chemistry of the three stones. The chemical composition was acquired by a ThermoFisher iCAP Q ICP-MS coupled with an Elemental Scientific Laser NWR213 laser ablation system. NIST 610 and 612 were used as external standards, and ^{27}Al was used as an internal standard. LA-ICP-MS results (see appendix 1 at https://www.gia.edu/doc/FA19-GNI-Appendix1.xls) showed that the three stones were predominantly composed of more than 90 mol.% gahnite ($ZnAl_2O_4$), with minor other end members of Al-spinel species. They should thus be classified as gahnites.

To better understand the composition of this type of spinel, we prepared a cross-section cut from the middle of one octahedral crystal, sample NBS3 (figure 4). A vertical line of 22 spots (figure 4, line 1) and a horizontal line of 22 spots (figure 4, line 2) were selected to cross the whole section from outer rims to the opposite outer rims for LA-ICP-MS analyses. All the spots showed more than 90 mol.% gahnite with hercynite as the second most abundant species (figure 5). Spots near the outer rims contained more hercynite than spots on the inner rims and core. The mol.% end member distribution was very consistent throughout the whole section. Nine trace elements for each spot in lines 1 and 2 were plotted in figure 5. In general, the outer rims had higher concentrations of V and Co but lower concentration of Ni than the inner rims and core.

Maxwell Hain and Ziyin Sun
GIA, Carlsbad

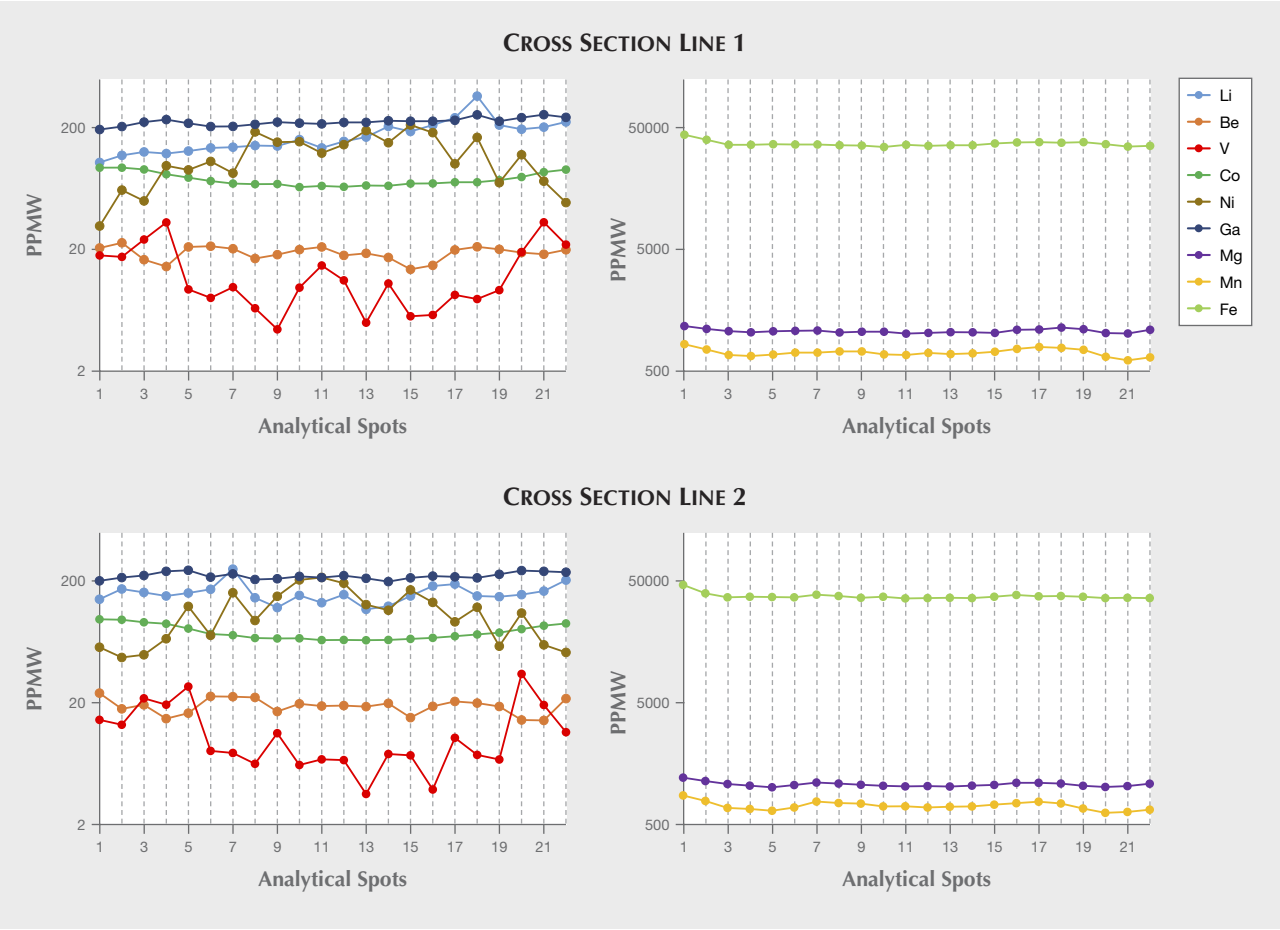

Figure 5. Trace element vs. position profiles revealed that the outer rims had higher concentrations of V and Co, but lower concentration of Ni than the inner rims and core. Detailed information on trace elements for each spot in lines 1 and 2 can be found in appendix 2 online (https://www.gia.edu/doc/FA19-GNI-Appendix2.xls).

Emerald update with Arthur Groom. At the 2019 AGTA GemFair in Tucson, Eternity Natural Emerald (Ridgewood, New Jersey) had emeralds up to 50 ct on display. Eternity's president, Arthur Groom, noted that the Afghanistan emerald melee sets (figure 6) had drawn the most interest. This rough melee is particularly attractive, he said, because of its higher brilliance than stones from other sources. "The Afghanistan melee is the brightest in its natural state when it's cut properly," he said. "Afghanistan emerald will rival Colombian any day of the week."

Figure 6. Melee goods from Eternity Natural Emerald. Photo by Kevin Schumacher.

Eternity has experimented with melee from different sources but finds Afghanistan melee the most plentiful and consistent. The company currently cuts Afghanistan emeralds in sizes from 1 mm to 70 ct, disproving the perception in the trade that the country produces only small emeralds. Groom pointed out that vibrant greens are not as easy to find in gems as other colors, and tsavorite is often used for green, but Eternity's emeralds offer the option to use one of the "Big Three" gemstones. Eternity also sources emerald rough from Ethiopia, Colombia, Brazil, and Zambia.

Cutting and mounting emerald melee has traditionally been challenging because of emerald's tendency for inclusions and fractures, and its typical enhancements. Most

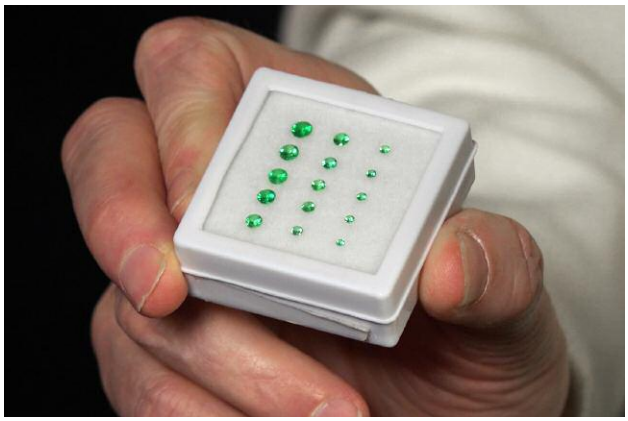

Figure 7. A set of 15 of Eternity Natural Emerald's calibrated emeralds ranging from 1 to 5 mm. Photo by Albert Salvato.

jewelry manufacturers do not like working with it, Groom said. Eternity has solved this problem after many years of effort, he said, producing "a finely made emerald that you can work with confidence and will never change." Eternity's enhancement process allows the stones to be cleaned in ultrasonic and steam cleaners with no adverse effects (traditional enhancement substances tend to alter over time).

Eternity has cut thousands of carats of rough and developed master sets of colors and clarities. They are able to fulfill orders for thousands of stones at a time. The emeralds are cut to exact proportions; the average weight retention is about 15 percent. "You can't be concerned with how much weight you'll lose," Groom said. In the past, manufacturers would buy a parcel of stones of different sizes, dimensions, and colors and find some stones unusable, but they can now buy stones of the same color, clarity, and size. Along with melee, the company offers cabochons and calibrated (figures 7 and 8) and faceted stones, in qualities from commercial-grade to very fine and at all price points. Groom showed us a set of calibrated emeralds (figure 8) ideal for a premium bracelet.

One of Eternity's aims is to promote Afghanistan emerald and country of origin. "The miner has to benefit from this," Groom said, "and this is one of our goals in Afghanistan." In our 2013 interview with Groom, he said Afghanistan's emerald resources are such that if the country were to see peace, acquire investors, and mechanize its mining operations, it would "outproduce the world."

Groom believes in promoting country of origin not because it adds value but because it adds identity to the stone. "We all know about Colombian emerald," he said. "But just because the emerald comes from Colombia doesn't make it more valuable. We just manufactured a 24 ct Tajik stone that sold for close to half a million dollars. You have to take the stone on its merit."

Duncan Pay and Erin Hogarth
GIA, Carlsbad

Figure 8. A set of calibrated emeralds (approximately 2 to 4 mm each) by Eternity Natural Emerald. Photo by Kevin Schumacher.

New find of deep blue aquamarine from Nasarawa State in Nigeria. The most unusual and exquisite things are often found in unexpected places. This has been seen in the explosion in gem discoveries in East Africa since the latter part of the twentieth century. However, West Africa has remained relatively underexplored, despite the development of some promising and productive gem deposits, including sapphire and Paraíba tourmaline in Nigeria. West Africa's gemological horizons expanded earlier this year with the find of a small batch of aquamarine with exceptionally deep and saturated color (figure 9). Reportedly found in Nasarawa State, the stones were recovered by small-scale artisanal miners whose workings reached only the near-surface exposure of a weathered pegmatite body. Mining was short-lived, starting likely in January and ending in May 2019, when the miners exhausted the surface deposit but lacked resources to continue with hard-rock mining once they hit bedrock. Through a local buyer in the Abuja market, author JH was able to obtain a large parcel that may account for the lion's share of the production from this deposit to date. This parcel amounted to 763 grams, of which 200 grams would cut stones over one carat.

Standard gemological testing showed properties consistent with aquamarine, with a uniaxial negative optic character, a refractive index of 1.582–1.590, a birefrin-

Figure 9. Nigerian aquamarine from a new find in Nasarawa State. The faceted stones range from 1.55 to 2.63 ct. Photo by Kevin Schumacher.

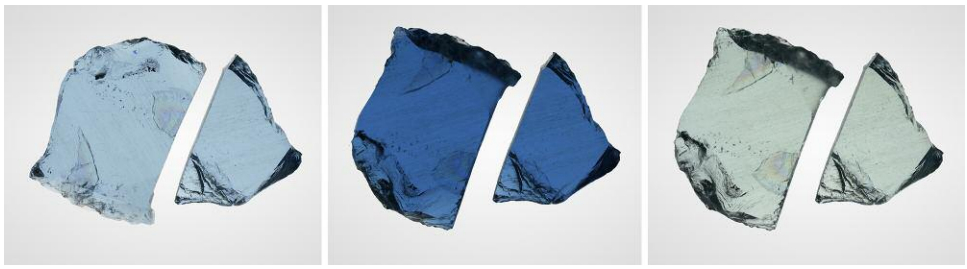

Figure 10. Two wafers of the new Nigerian aquamarine in unpolarized light (left), and with light polarized along the extraordinary ray (center) and along the ordinary ray (right). Photos by Aaron Palke.

gence of 0.008, and a specific gravity of 2.71–2.73. The stones were inert under short-wave and long-wave UV light. The most exceptional feature of this new find of aquamarine—besides its attractive, saturated blue color—is its unusually strong pleochroism, going from deep, saturated blue with light polarized parallel to the extraordinary ray to an unsaturated (almost colorless) greenish blue with light polarized parallel to the ordinary ray (figure 10). The origin of this extreme pleochroism is seen in the UV-Vis spectra (figure 11), in which the main feature is a highly polarizable broad absorption band at approximately 680 nm caused by Fe^{2+}-Fe^{3+} intervalence charge transfer (IVCT). This IVCT absorption is the cause of blue coloration in (non-Maxixe) aquamarine (e.g., I. Adamo et al., "Aquamarine, Maxixe-type beryl, and hydrothermal synthetic blue beryl: Analysis and identification," Fall 2008 *G&G*, pp. 214–226). Also seen are an absorption band at 835 nm related to octahedral Fe^{2+} and narrow absorption bands at 372 and 428 nm related to octahedral Fe^{3+}. The reason for the intense pleochroism is simply the increased intensity of the highly polarizable Fe^{2+}-Fe^{3+} IVCT chromophore relative to most other aquamarine. Note that the two wafers in figure 10 were cut from the same piece of rough and were used in a pilot heat treatment experiment. The larger one on the left was not heated, while the smaller piece on the right was heated at 400°C for two hours, with no apparent change in its color or appearance. It is not clear, however, if any of the material had been heated before it reached the market; further experiments may be warranted.

Microscopic observations showed an abundance of highly reflective, opaque, elongate needles and platelets that appeared light brown to black in darkfield and transmitted light (figure 12). Confocal Raman spectroscopy could not isolate the inclusions, but their dark color and reflective nature suggest they might be Fe oxides, which would be consistent with the iron-rich nature of these stones.

Figure 11. UV-Vis-NIR absorption spectra of a polished plate of Nigerian aquamarine showing both the ordinary (o-ray) and extraordinary (e-ray) ray absorption.

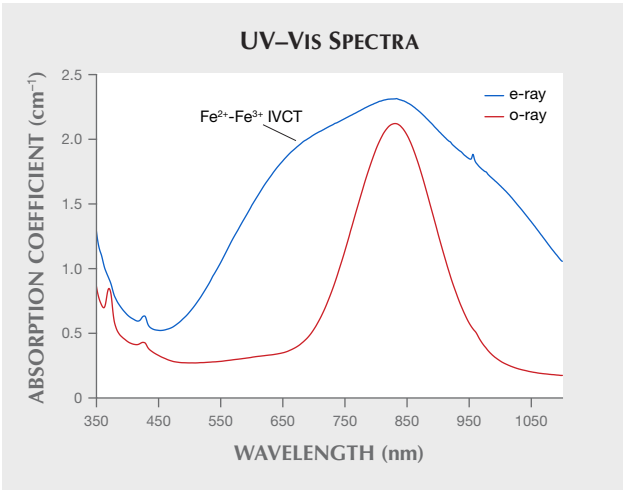

Figure 12. Needle and platelet inclusions are ubiquitous in this new find of Nigerian aquamarine, as seen with transmitted light polarized along the o-ray (top) and e-ray (bottom). Photomicrographs by Nathan Renfro; field of view 1.43 mm.

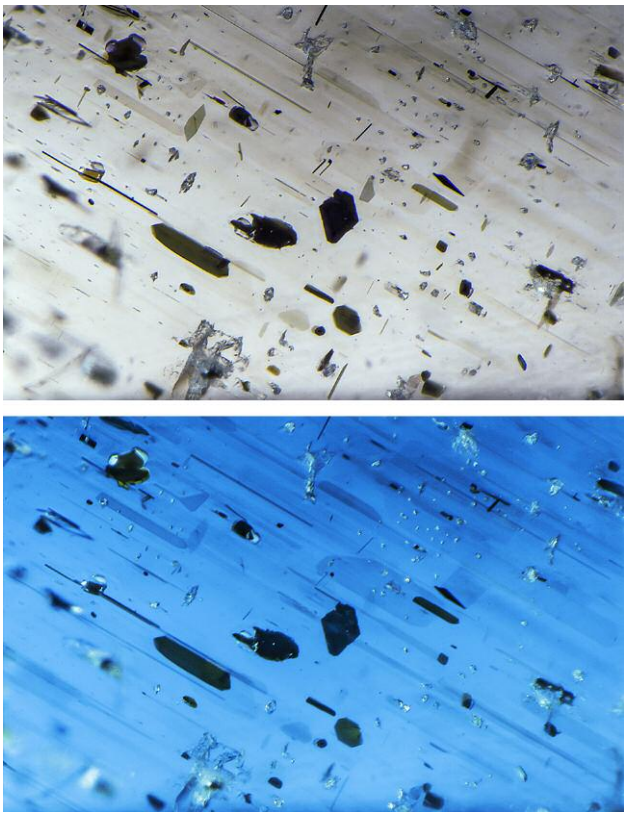

TABLE 1. Trace element chemistry (in ppmw) of Nigerian aquamarine from Nasarawa State.

	^{7}Li	^{23}Na	^{24}Mg	^{39}K	^{43}Ca	^{47}Ti	^{51}V	^{53}Cr	^{55}Mn	^{57}Fe	^{69}Ga	^{85}Rb	^{133}Cs
Average	434	8870	7900	1530	230	16	110	24	221	12000	32	183	905
Range	383–491	8530–9400	7620–8200	1440–1650	208–262	15–19	100–116	4–49	183–272	11000–12600	29–36	161–205	555–1450
Detection limits	0.02	1.1	0.09	0.2	4.3	0.1	0.01	0.1	0.02	0.6	0.004	0.003	0.01

Trace element content of the Nigerian aquamarines was measured by LA-ICP-MS (table 1). They were extremely enriched in alkali metals, especially Li, K, and Na (up to 9400 ppm). To the authors, these high concentrations of alkali metals seem unusual for gem-quality aquamarine among global deposits (including saturated material from Santa Maria in Minas Gerais, Brazil). The unique chemistry of this new material almost warrants the use of the term "alkali beryl," even though this term is nonstandard in the mineralogical community. Also notable is the relative enrichment of Cr from 4 to 49 ppm, compared to around 1 ppm Cr or less in aquamarine from most other deposits. The Cr enrichment was also indicated by the prominent Cr fluorescence measured by photoluminescence spectroscopy. Finally, the deep blue color of these stones was explained by their relative enrichment in Fe from 11,000 to 12,600 ppm. Such a high concentration of Fe increases the probability of having adjacent Fe^{2+} and Fe^{3+} cations, thereby facilitating and enhancing the Fe^{2+}-Fe^{3+} IVCT interaction. For now, this new deposit of fine Nigerian aquamarine lies dormant, but the world awaits the next important gem discovery in West Africa.

Aaron C. Palke
GIA, Carlsbad

Jeffrey Hapeman
Earth's Treasury, Westtown, Pennsylvania

A near-round natural pearl discovered in the edible oyster *Magallana bilineata*. Pakistan, which has a coastline stretching 1,046 km (650 miles) along the Arabian Sea, the Indian Ocean, and the Gulf of Oman, is blessed with numerous marine resources, including oysters that mainly inhabit estuaries and mangrove habitats. In Sindh Province, some oyster reefs at Hab River Delta have high ecological and economic value. Nine edible oyster species belonging to the genera *Crassostrea*, *Saccostrea,* and *Ostrea* have been recognized from different localities there. Pearl-forming mollusks belonging to the genera *Pinctada* have been reported from Daran Beach.

The Ostreidae family includes edible oysters and is most commonly known as a source of seafood (K. Scarratt et al., "A note on a pearl attached to the interior of *Crassostrea virginica* [Gmelin, 1791] (an edible oyster, common names, American or Eastern oyster)," *Journal of Gemmology*, Vol. 30, No. 1-2, 2006, pp. 43–50). Of these, *Magallana bilineata* has the widest distribution in the Indo-Pacific region, encompassing the coasts of northern Arabia, the Bay of Bengal, the Andaman Sea, the Java Sea, South China and Vietnam, the Philippines, and Okinawa.

Magallana bilineata is a euryhaline species that inhabits backwaters, creeks, estuary banks, coastal bays, and lagoons, forming oyster beds on a large scale. A large number of specimens of this species from Hab River Delta were examined to study the taxonomic characteristics of the genus *Magallana* as part of a joint project between Japan and Pakistan. Ten shells of each species were opened. Only one shell of *M. bilineata* (150 mm shell height) contained a pearl, attached to tissues near the adductor muscle. It was near-round, with a smooth surface and a purplish and off-white color very similar to the inner shell layer of *M. bilineata* (figure 13, left). The crystal structure of calcium carbonate was observed under high magnification. The non-nacreous, shiny pearl (figure 13, right) was 4.15 mm in diameter and weighed 0.02 g. The specimen is housed at the Centre of Excellence in Marine Biology, University of Karachi (part of the study collection of author SA).

Oysters living in tropical and warm regions have darker, more vivid, and more extensive coloration than

Figure 13. The inner and outer shell of M. bilineata *(left and center). A near-round pearl (right) was found inside the shell. Photos by Sadar Aslam.*

those in cooler climates. Our finding is very similar to that of Scarratt et al. (2006), which found a pearl inside *Crassostrea virginica* that was attached to an adductor scar. In our case, the pearl was attached to the tissues near an adductor scar. This finding demonstrates the very rare phenomenon of edible oysters producing natural pearls. However, further work will be needed to determine its chemical composition using highly accurate analytical methods.

Sadar Aslam, Malik Wajid Hussain Chan, Ghazala Siddiqui, and Syed Jamil Hasan Kazmi
University of Karachi, Pakistan

Noman Shabbir
PTV News, Karachi

Tomowo Ozawa
Nagoya Biodiversity and Biosystematics Laboratory, Nagoya, Japan

Natural sapphire with trapiche pattern inclusions. A blue gemstone pendant was recently submitted to Guild Gem Laboratories for identification. Standard gemological testing identified it as a sapphire, with a refractive index of 1.762–1.770 and birefringence of 0.008. Fourier-transform infrared (FTIR) spectroscopy combined with microscopic observation confirmed it was a natural sapphire. The UV-Vis spectrum indicated a basalt-related origin owing to relatively high iron content. The FTIR transmitted spectrum also revealed a 3309 series with peaks at 3366, 3309, 3232, and 3185 cm^{-1}, which are commonly seen in basalt-related sapphire.

Figure 14. The regular hexagonal inclusions consisted of six independent units, resembling a trapiche pattern. Photomicrograph and illustration by Yizhi Zhao; field of view 1.70 mm.

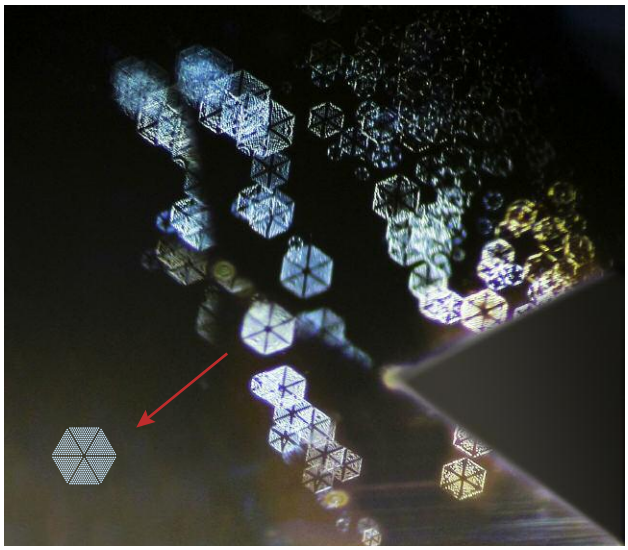

Microscopic observation showed several colorless crystals and fluid inclusions under reflective and transmitted light. Using a fiber-optic light, we also observed very interesting scenes of whitish clouds (figure 14) consisting of arrays of hexagonal particles. These particles seemed to be flat and parallel to each other. A distinct uniaxial interference pattern was observed when viewing perpendicular to these particles under the polariscope equipped with a conoscope, which proved that they were parallel to the basal plane (0001) crystalline face of corundum. Further observations revealed that each particle possessed six nearly identical triangular sectors, divided by six arms with hexagonal symmetry. Based on our microscopic observation and estimation, the diameters of the hexagons ranged from approximately 0.06 to 0.13 mm. This pattern was very similar to the trapiche structure seen in some sapphire, ruby, and emerald.

The depth of the inclusions prohibited Raman spectroscopy testing, but we will monitor this phenomenon in other samples for further study in the future.

Yujie Gao, Dan Ju (judan@guildgemlab.com), and Yizhi Zhao
Guild Gem Laboratories, Shenzhen, China

Opals revisited. In the 1980s, the author and his wife, Corky, acquired large quantities of Virgin Valley "wet" opal specimens displayed in glass domes with water and other specimens immersed in silicone oil. The domes had black rubber stoppers on the bottom. The mine representative had put them in water and silicone oil to enhance their beauty, since wetting the surface gives the illusion of a polished gem specimen.

Opal is a hydrated amorphous silica, and those with a high water content tend to craze and crack if left to dry. If a specimen is inclined to craze or crack, placing it in a liquid does not stabilize it or heal the cracks within, but it does delay the "day of reckoning" when the opal eventually deteriorates.

The specimens displayed in the domes with water began forming deposits, and within months the water became cloudy and the domes were crusted with precipitate from dissolved minerals. Those in silicone oil fared better, but eventually they too deteriorated, with the silicone oil taking on a yellow cast from the black rubber stoppers, which appeared to coat the opals with a yellow crust (figure 15).

After years of changing the water and silicone oil, the cleaning and repackaging eventually became very time-consuming. The author removed all the wet specimens from their domes, cleaned and wrapped them in paper towels, and put them in boxes. The boxes with the now-dry opal specimens were packed away and stored in the garage, where they remained for more than 27 years.

In July 2019, the author found the boxes containing these beautiful and long-forgotten opals. The results were astonishing. They had not fallen apart, and they looked more stable than they had when dried and put away. The cracks were

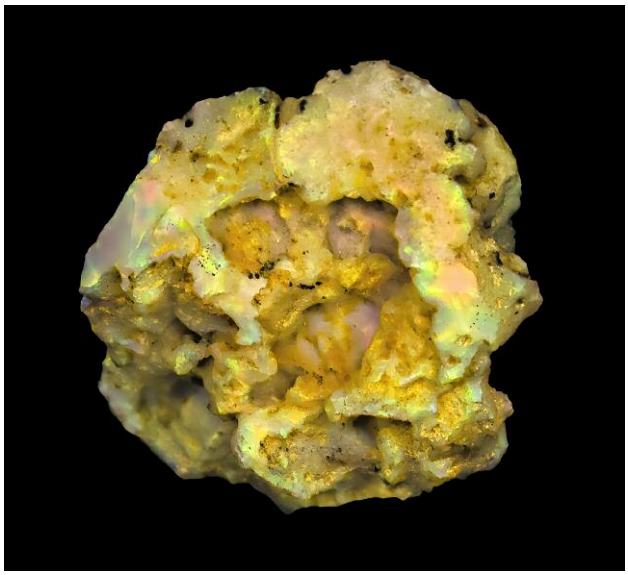

Figure 15. The untouched opal specimen displays the yellow coating caused by years of storage in silicone oil. Photo by Ted Grussing.

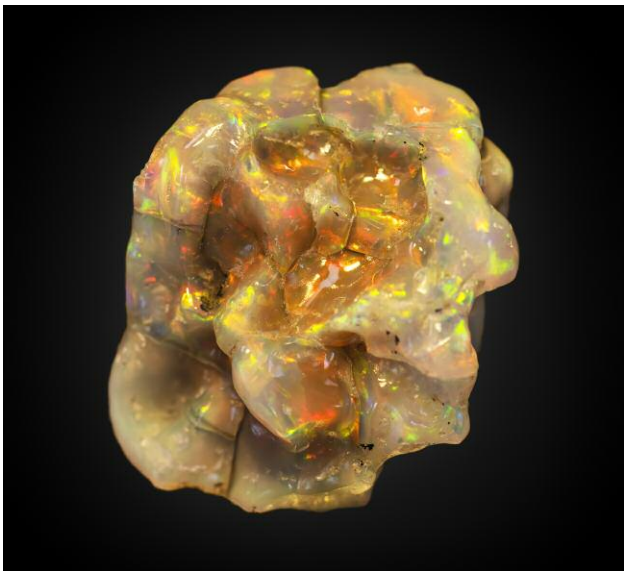

Figure 17. The finished piece, dry and ready for display. Photo by Ted Grussing.

still there, but the look was different. They looked like they could be worked—if not on the wheels, then with a flex shaft. The first opal that caught the author's eye (again, see figure 15) was cleaned and worked (figure 16). The completed piece, shown in figure 17, is named "Bonnie Jean." There are many more to finish, and they are dry and unlikely to craze or crack any further.

Ted Grussing
Sedona, Arizona

Trapiche emerald from Swat Valley, Pakistan. Trapiche emeralds are usually found in Colombia. Recently the authors received six emeralds reportedly from Swat Valley, Pakistan, polished as double-sided wafers, retaining their original hexagonal crystal habit and exhibiting a trapiche-like pattern (figure 18). These samples weighed from 0.38 to 0.83 ct, with a refractive index of 1.588–1.599 and a birefringence of 0.009–0.011.

Generally, these trapiche emeralds were composed of four parts from rim to core: a green rim, a light green area, six arms, and a colorless core, as illustrated in figure 19A. The rims had a highly saturated green color, and most were relatively clean except for several fractures and tiny fluid inclusions. The rims ranged from approximately 1 to 2 mm wide. Although the boundary between the green rim and

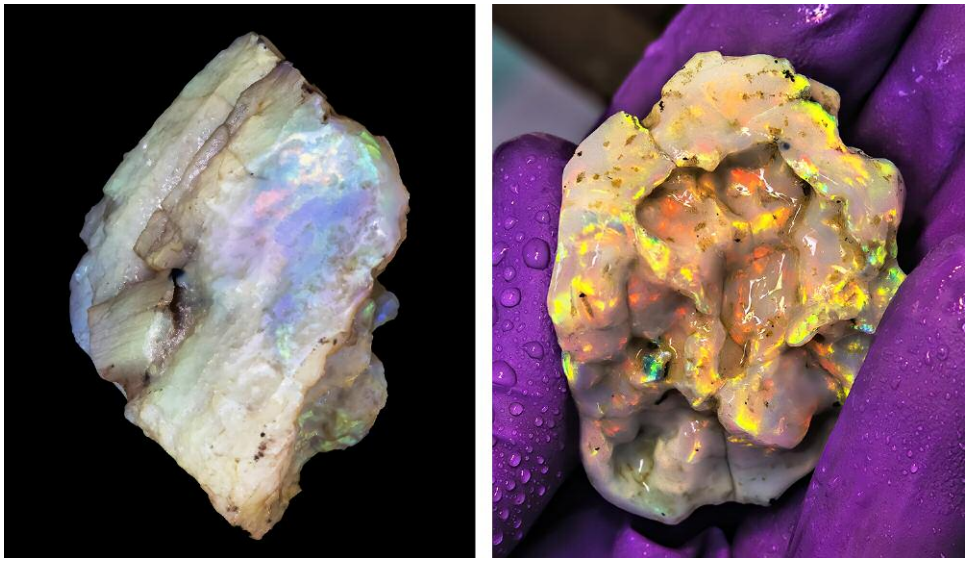

Figure 16. Left: The side of the specimen after cleaning and rubbing on a diamond wheel. Right: The nearly finished opal midway through the cleaning process. Photos by Ted Grussing.

Figure 18. Six emerald wafers reportedly from Swat Valley, Pakistan, showing a trapiche-like pattern. They range from 0.83 to 0.38 ct from left to right, with a thickness of about 1.51 to 2.08 mm. Photo by Kaiyin Deng.

the light area was not very sharp, a hexagonal boundary was visible. Six black arms spread in a hexagonal symmetric pattern, with each arm perpendicular to the hexagonal side. The colorless core usually had a hexagonal shape.

Microscopic observation revealed that every arm contained many minute black platy inclusions. These small particles appeared dark under transmitted light (figure 19B), while they showed bright metallic luster under reflected light (figure 19C). Micro-Raman analyses (figure 20) identified these inclusions as magnetite. Peaks at 662 and 545 cm^{-1} were consistent with two main peaks of magnetite, according to the RRUFF online database (rruff.info), while peaks at 683 and 400 cm^{-1} may be assigned to the emerald host. Chemical analysis by energy-dispersive X-ray fluorescence (EDXRF) on the sample shown in figure 19 revealed an iron content of 20,860 ppm (n = 3) in the light green area and 17,000 ppm (n = 3) in the rim. The difference in iron content may be due to the inclusions, since magnetite (Fe_3O_4) is mainly composed of iron and oxygen.

To our knowledge, there have not been many reports of trapiche emerald from localities other than Colombia.

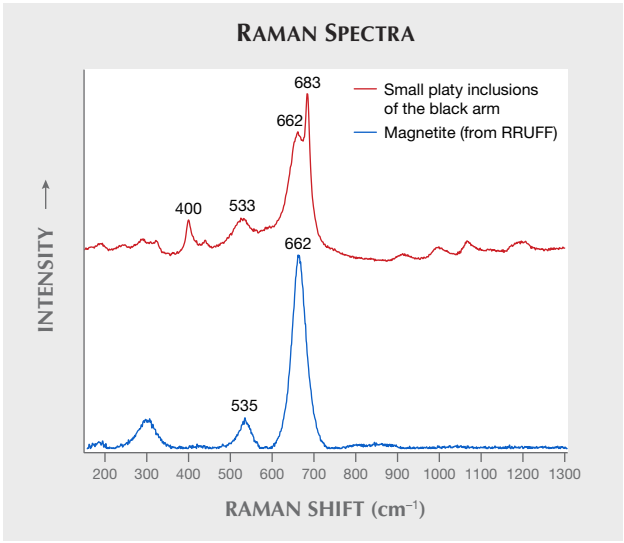

Figure 20. Raman analysis identified these inclusions as magnetite. Peaks at 662 and 545 cm^{-1} agree with the two main peaks of magnetite, according to the RRUFF database, while peaks at 683 and 400 cm^{-1} may be assigned to the emerald host.

The trapiche pattern caused by platy magnetite inclusions could help advance our understanding of trapiche.

Yujie Gao, Xueying Sun (shirley.sun@guildgemlab.com), and Mengjie Shan
Guild Gem Laboratories, Shenzhen, China

Uvarovite in prehnite from Pangasinan Province, Philippines. Uvarovite, $Ca_3Cr_2(SiO_4)_3$, is the rarest of the commonly encountered garnet species, and the only one that is consistently green. Although seldom faceted due to its tendency to be opaque, drusy coatings of tiny bright green uvarovite crystals on chromite matrix from Russia are used for jewelry. Recently, a new type of rock with lapidary po-

Figure 19. The trapiche emeralds from Pakistan were mainly composed of four parts: a green rim, a light green area, six arms, and a nearly colorless core as illustrated in figure A. These arms appear dark under transmitted light (B) and show bright metallic luster under reflected light (C); field of view 8.48 mm. Illustration and photos by Yujie Gao.

Figure 21. This new ornamental gem material from the Philippines consists of vibrant green uvarovite garnets in a white prehnite matrix. The polished freeform weighs 4.23 ct. Photo by Robison McMurtry.

tential was reportedly discovered in the Philippines, consisting of a white prehnite matrix with vibrant green crystals of uvarovite (figure 21).

This new material was brought to the authors' attention by Xavier A. Cortez, who operates Crystal Age, a gem shop in Quezon City. While attempting to source jade for his shop in early 2019, Xavier was offered unidentified white stones speckled with bright green crystals from local miners on the island of Luzon. Mr. Cortez was able to track down the source of this material to a rural portion of Pangasinan Province, in the Ilocos region of Luzon. Weathered calc-silicate rocks at this deposit yield small euhedral crystals of opaque bright green garnets as well as compact green masses in white matrix. The measured spot refractive index of 1.63 was consistent with prehnite. The identities of the green uvarovite and the white prehnite matrix were confirmed with Raman spectrometry.

While there is currently very little of this material on the market, it could be used as a jadeite simulant due to its mottled white and green appearance. Aside from its potential as a jadeite simulant, it is an interesting ornamental material that can be appreciated for its own unique beauty and vibrant green color.

Ian Nicastro
San Diego, California
Nathan Renfro
GIA, Carlsbad

DIAMONDS

The Rare Sun diamond. While manufacturers typically seek to minimize or remove inclusions in gem-quality diamonds, a few are specifically cut to highlight these features. Certain hydrogen-rich diamonds can yield fascinating inclusion forms when faceted. One such stone is the 5.24 ct Rare Sun diamond (figure 22), which GIA's New York laboratory recently had the opportunity to examine. Framed at the center of this Fancy Dark yellowish brown modified octahedron is an eye-visible cloud inclusion that scatters light to form the image of a star and its shining rays. The inclusion's orientation gives it an unusually distinct six-fold symmetry, which is very rare. The overall shape of the Rare Sun diamond has been precisely polished so that as light touches various parts of its surface, a different ray beams through. Achieving this effect required extremely precise fashioning—even the slightest error in cutting or polishing would have diminished the effect.

Very few diamonds have the potential to display this star-like pattern, and fewer still ever have this potential recognized and achieved. Diamonds with unusual inclusions, especially inclusions that suggest the shape of other objects, are also prized by gem collectors and seekers of the uncommon. The Rare Sun diamond is a large and noteworthy example and could be considered among those unique diamonds.

This diamond, with its particularly distinctive inclusion scene, also serves as a valuable research material. Gemologists welcome the opportunity to study gems with such unusual features.

Manoj Singhania and Apoorva Deshingkar
GIA, Mumbai

SYNTHETICS AND SIMULANTS

Artificial glass imitating blue amber. Artificial glass, a low-cost material, is capable of simulating any gemstone owing to its range of appearances (bodycolor, transparency, and

Figure 22. The Rare Sun diamond, a 5.24 ct Fancy Dark yellowish brown modified octahedron, has a centrally located, eye-visible inclusion resembling a star and its rays. Photo by Jian Xin (Jae) Liao.

Figure 23. This 139.34 ct piece of artificial glass bore a striking similarity to blue amber. Photo by Lai Tai-An Gem Lab.

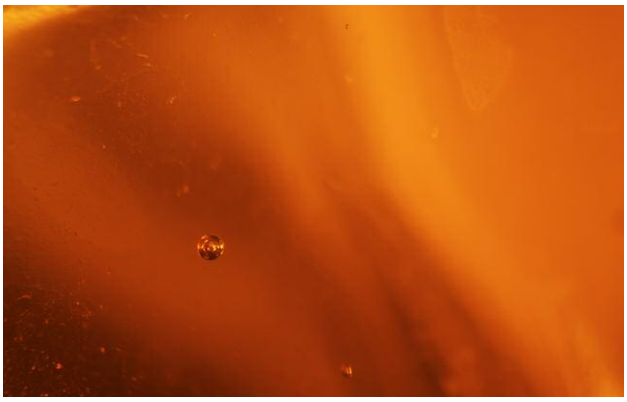

Figure 24. Examination with a gemological microscope revealed gas bubbles. Photomicrograph by Lai Tai-An Gem Lab; field of view 2.6 mm.

phenomena). While this material is usually straightforward to identify, in some cases it is visually similar to the gem material being imitated. The Lai Tai-An Gem Laboratory recently received an object for identification that the client claimed was blue amber, but was subsequently determined to be artificial glass (figure 23).

The transparent, irregularly shaped, brownish yellow object with a bluish surface-related effect and vitreous luster weighed 139.34 ct and measured 37.0 × 33.2 × 28.6 mm. While it closely resembled amber, its heft was completely at odds with that expected for an amber of its size, providing the first important clue about its identity. Standard gemological testing revealed a spot refractive index of 1.50, a specific gravity of approximately 2.50 (amber's is 1.08), a weak chalky blue reaction under short-wave ultraviolet radiation, and an inert response to long-wave UV. Inspection with a gemological microscope revealed gas bubbles (figure 24). Standard gemological testing confirmed that the item was not amber but artificial glass, though more advanced analysis was carried out. Fourier-transform infrared (FTIR) spectrometry was consistent with data we obtained on some samples of known glass (figure 25), confirming the identity. Energy-dispersive X-ray fluorescence (EDXRF) spectrometry also detected Si and Pb as the main chemical elements.

Blue amber's optical effect, produced by the extremely shallow blue fluorescence stimulated by UV light, is strictly confined to the surface. A strong blue fluorescence under long-wave UV radiation is also typical in such amber, so the inert reaction also indicated the material's artificial nature. The object exhibited a similar optical effect when viewed at different angles or when the direction of illumination changed.

In our experience, it is uncommon to see this type of artificial glass imitating blue amber. The gas bubble inclusions, while typical of glass, may also be encountered in amber, so additional gemological analysis may be neces-

Figure 25. Comparison of the infrared spectra for amber (red trace, collected by the author) and the artificial glass imitation (blue trace). The absorption at 1077 cm^{-1} is assigned to artificial glass.

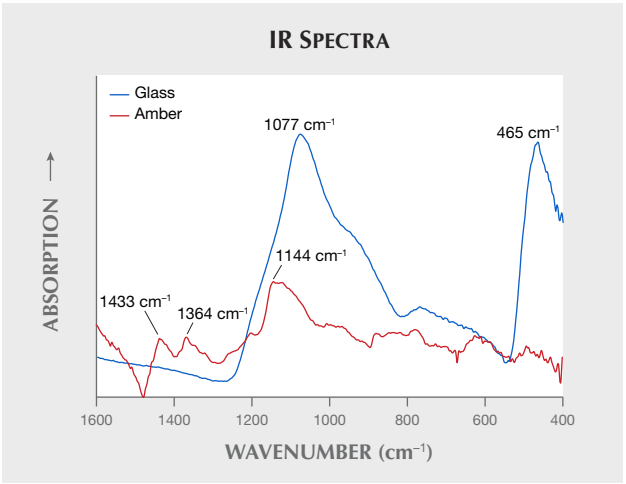

Figure 26. Two near-round beads cut from shell, 9.22 × 9.15 × 8.67 mm (left, 5.04 ct) and 9.51 × 9.44 × 8.69 mm (right, 5.45 ct). Photo by Hasan Abdulla.

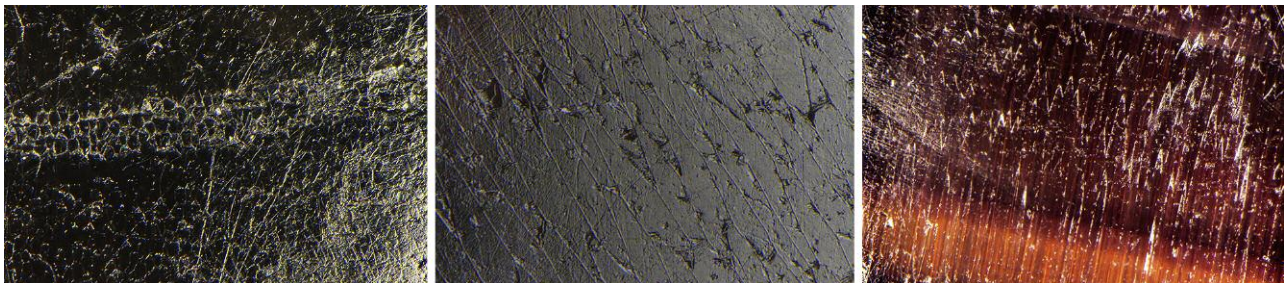

Figure 27. Columnar structures observed in the smaller bead made of calcite (left, reflected light) and elongated structures made of aragonite (center, reflected light) due to fibrous crystals of aragonite (right, reflected and transmitted light). Similar structures were also observed on the larger bead. Polish lines are observed in all images. Photomicrographs by Hasan Abdulla; fields of view 1.5 (left), 1.1 (center), and 2.4 mm (right).

sary to ensure the correct identification. This case clearly illustrates how artificial glass can imitate virtually every gemstone imaginable and mislead the unwary bargain hunter.

Larry Tai-An Lai (service@laitaian.com.tw)
Lai Tai-An Gem Laboratory, Taipei

Black non-nacreous pearl imitations made of beads cut from shell. DANAT (Bahrain Institute for Pearls & Gemstones) recently received a 5.04 ct bead (9.22 × 9.15 × 8.67 mm) and a 5.45 ct bead (9.51 × 9.44 × 8.69 mm), both of near-round shape (figure 26). Under the microscope, both beads presented columnar structures in some areas, similar to those observed in some non-nacreous pearls (N. Sturman et al., "Observations on pearls reportedly from the Pinnidae family (pen pearls)," Fall 2014 *G&G*, pp. 202–215), as well as elongated structures due to fibers reaching the surface (figure 27). Raman spectra with a 514 nm green laser were difficult to acquire, as they revealed high luminescence possibly linked to their high organic matter content; however, there was enough Raman signal to be able to identify calcite and aragonite. The calcium carbonate identification was confirmed by acquiring FTIR reflectance spectra. In the Raman spectra, weak bands linked to polyenic pigments were also observed.

Chemical analysis of the beads using energy-dispersive X-ray fluorescence (EDXRF) did not show any measurable manganese. Strontium was above 800 ppmw, and they remained inert under X-ray imaging, similar to saltwater pearls. Digital X-ray microradiographs and micro-CT did not show any internal structures.

Under long-wave and short-wave ultraviolet light, zoned/banded/layered fluorescence was observed (figure 28). Using transmitted fiber-optic illumination, banded structures and fibrous structures were visible with the unaided eye (figure 29). These characteristics were similar to those observed in imitation pearls made of non-nacreous shell material. Most of the imitation pearls described previously had a light color or were artificially dyed. The beads examined in this study, though, presented no evidence of any color treatment under the microscope or

Figure 28. Reaction of the beads under long-wave UV (top) and short-wave UV (bottom). Note the luminescence distribution in the different zones. Photos by Hasan Abdulla.

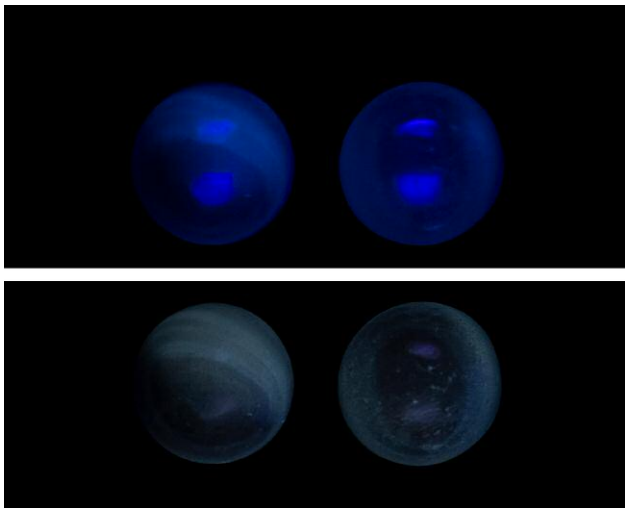

Figure 29. Under transmitted fiber-optic illumination, the 5.04 ct bead displayed a banded structure reminiscent of beads cut from the inner part of a shell. Photo by Hasan Abdulla.

Figure 30. This opal imitation shows a billowy play-of-color phenomenon. The largest block measures approximately 61.79 mm in length. Photo by Robison McMurtry and Diego Sanchez. Courtesy of Sanwa Pearl & Gems Ltd.

using EDXRF and Raman spectroscopy. The "zoned" fluorescence reaction under UV light was linked with different structures and not with the artificial colorants.

Large white beads with fibrous aragonite supposedly cut from bivalves from *Tridacna* species, which contain thick inner layers, have previously been used to imitate pearls (Summer 2004 GNI, p. 178; Summer 2006 Lab Notes, pp. 166–167; M. Krzemnicki and L. Cartier, "Fake pearls made from *Tridacna gigas* shells," *Journal of Gemmology*, Vol. 35, No. 5, 2017, pp. 434–429). These beads were sometimes dyed to alter their coloration. A salmon-colored bead of about 10 mm, supposedly cut from the inner part of *Lobatus gigas*, was used to imitate coral (E. Disner and F. Notari, "Gastropod shell beads disguised in a coral necklace," *Journal of Gemmology*, Vol. 34, No. 7, 2015, pp. 572–574). The beads we examined were of natural black color, and we are still looking for a mollusk that might have a non-nacreous inner shell layer where beads of that size could be cut.

Acknowledgments: The authors would like to extend their appreciation to Mr. Saud Bin Rajab (Manama, Bahrain) for allowing us to publish the study on these beads.

Stefanos Karampelas (Stefanos.Karampelas@danat.bh), Ali Al-Atawi, Hasan Abdulla, Bader Al-Shaybani, and Fatema Almahmood
DANAT (Bahrain Institute for Pearls & Gemstones)
Manama, Bahrain

Imitation opal with interesting play-of-color pattern. GIA's Carlsbad laboratory recently examined samples of a relatively new manufactured gem material sometimes known as a "hybrid opal product" (figure 30) (see Spring 2018 Lab Notes, pp. 60–62). This material showed a refractive index of 1.498–1.500, and the specific gravity ranged from 1.33 to 1.35. Both of these properties fall far outside the range for natural opal, making identification very straightforward for the gemologist. These anomalous gemological properties also mean that this material is best described as an opal imitation and not a synthetic opal. This material is reportedly composed of about 20% silica and about 80% resin, which is consistent with the gemological properties measured.

This new imitation opal showed a pronounced play-of-color phenomenon with a pattern unlike the kind one would expect to see in conventional synthetic opal. Instead of small cellular patches, it displayed broad swaths of ever changing play-of-color covering large areas of the surface (figure 31). The laboratory examined samples that showed

Figure 31. The imitation opal showed broad swaths of the play-of-color phenomenon when examined with a microscope. Photomicrograph by Nathan Renfro; field of view 18.80 mm.

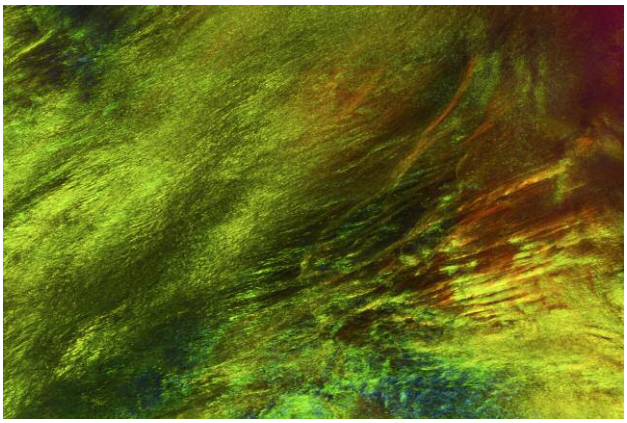

Figure 32. Thermal enhancement and unusual inclusions were detected in this 2.05 ct blue sapphire, measuring 7.07 × 6.55 × 4.99 mm. Photo by Kaiyin Deng.

either a black or white bodycolor and a variety of colors in the play-of-color areas. For those who love opal, this attractive material could offer a cost-effective alternative to natural material while retaining the allure of the play-of-color phenomenon.

Nathan Renfro

TREATMENTS

Dendritic inclusions of thorianite in heated blue sapphire. Recently, a 2.05 ct blue sapphire was sent to Guild Gem Laboratories for identification (figure 32). Standard gemological testing confirmed it was corundum, with a refractive index of 1.762–1.770 and specific gravity of 4.00. Under microscopic observation, cloudy particles and diffuse straight color zoning were seen, as well as fingerprint-like fluid inclusions as shown in figure 33, indicating that this stone had undergone thermal enhancement. This sapphire exhibited chalky greenish fluorescence around the girdle under short-wave (254 nm) ultraviolet fluorescence light. Further UV-Vis spectroscopic testing suggested a metamorphic origin, while FTIR spectra (figure 34) showed a distinct 3309 series at 3185, 3232, 3309, and 3367 cm^{-1}, confirming heat treatment. Energy-dispersive X-ray fluorescence (EDXRF) showed an Fe content around 300–500 ppm. Neither U nor Th was detected.

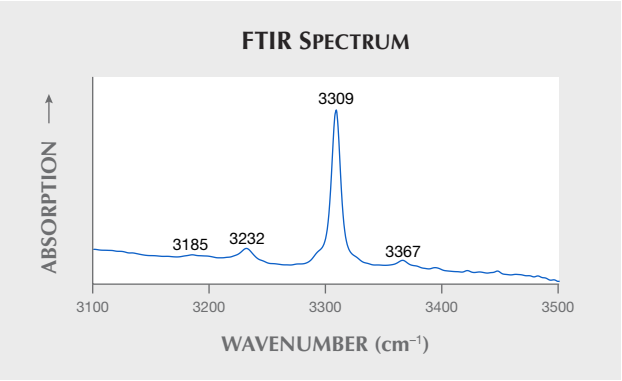

Figure 34. The sapphire's FTIR spectrum exhibited a distinct 3309 series at 3185, 3232, 3309, and 3367 cm^{-1}.

Also observed were interesting dendritic inclusions, which are not very common in sapphire. These inclusions showed relatively strong metallic luster under reflected light, and they appeared to be opaque under transmitted light. Lines of small dots were seen under higher magnification. These dot-like inclusions exhibited a blurred surface and a rounded shape. Raman analysis at the National Gemstone Testing Center (NGTC) using a 473 nm laser showed three distinct peaks at 466, 552, and 607 cm^{-1}, matched very well with thorianite, according to the RRUFF online database (rruff.info), as shown in figure 35. Thorianite (ThO_2) is an oxide mineral mainly composed of Th and O, first found in an alluvial deposit in Sri Lanka (D.

Figure 33. Left: Dendritic inclusions consisted of dot-like minerals showing a "melted and diffused" appearance. Photo by Yujie Gao; field of view 2.68 mm. Center: Resembling a tree root, these dendritic inclusions showed relatively strong metallic luster under reflected light. Photo by Yizhi Zhao; field of view 2.52 mm. Right: Dendritic inclusions coupled with blurred blue color zoning. Photo by Yujie Gao; field of view 9.73 mm.

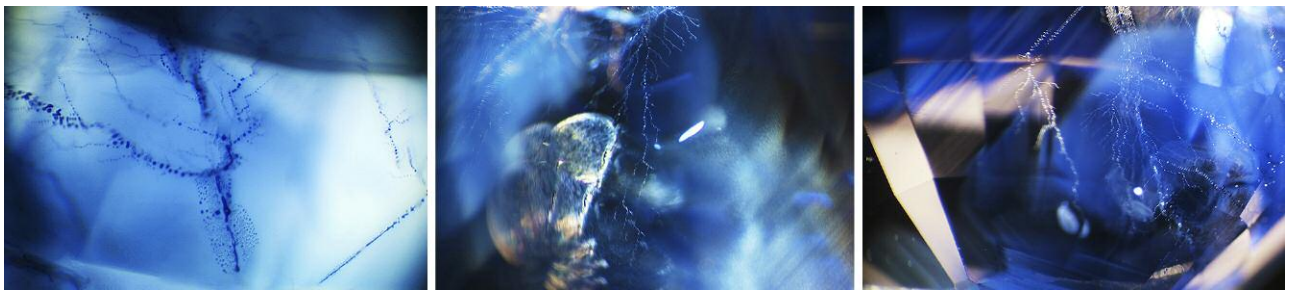

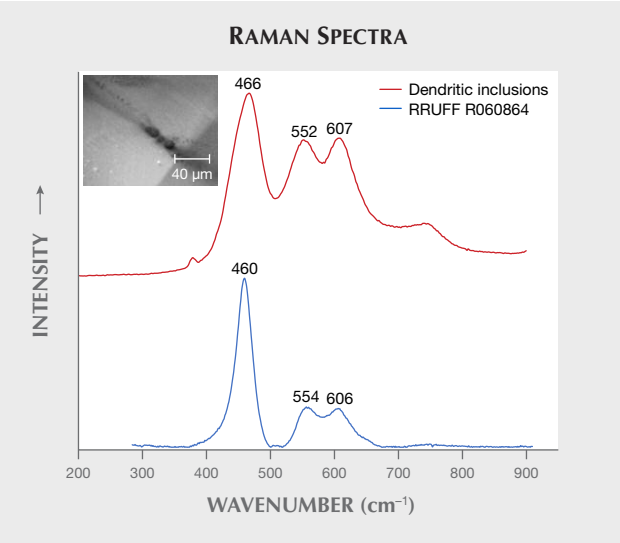

Figure 35. Raman spectra of the sapphire's dendritic inclusions matched with thorianite (ThO_2).

Wyndham, "The occurrence of thorium in Ceylon," *Nature*, Vol. 69, 1904, pp. 510–511). A melted appearance of a mineral inclusion and/or unnatural-looking discoid fractures around inclusions can be indicative of heat treatment in corundum. Such phenomena are normally attributed to the breakdown of mineral inclusions at high temperature. However, the thorianite inclusions here did not have the typical appearance of inclusions that have been altered by high-temperature heat treatment. The diffuse appearance of thorianite is unlikely to be an indicator of heat treatment. Further experiments and tests on thorianite in unheated sapphire would give us more clues in the future.

Yujie Gao (peter.gao@guildgemlab.com) and Xueying Sun
Guild Gem Laboratories, Shenzhen, China

Huihuang Li
National Gemstone Testing Center (NGTC)
Shenzhen, China

Recrystallization of baddeleyite as an indicator of PHT ("HPHT") treatment in sapphire. PHT ("HPHT") treatment in sapphire has been a controversial topic the last few years. Recently, Guild Gem Laboratories in Shenzhen received a 7.11 ct blue sapphire (figure 36) for identification. The refractive index of 1.762–1.770 and hydrostatic specific gravity of 4.00 confirmed the stone's identity. It was inert under long-wave and short-wave UV. Microscopic examination revealed several distinct features, such as diffuse color bands and melted white solid mineral inclusions surrounded by discoid fractures, indicating that this stone had undergone thermal enhancement (figure 37).

Further UV-Vis spectroscopic testing specified a metamorphic geological origin, while energy-dispersive X-ray fluorescence (EDXRF) analysis revealed low Fe content around 400–600 ppm. FTIR spectra (figure 38) showed a

Figure 36. This 7.11 ct oval blue sapphire, measuring 11.66 × 10.44 × 7.38 mm, exhibits eye-visible white mineral inclusions. Photo by Yizhi Zhao.

distinct 3309 cm^{-1} series at 3181 and 3373 cm^{-1}, consistent with heated metamorphic sapphire. We also noticed a broad band centered at 3042 cm^{-1}, accompanied by peaks at 2627, 2412, 2349, 2319, and 2096 cm^{-1}. According to previous reports (S.-K. Kim et al., "Gem Notes: HPHT-treated blue sapphire: An update," *Journal of Gemmology*, Vol. 35, No. 3, 2016, pp. 208–210; A. Peretti et al., "Identification and characteristics of PHT ('HPHT') - treated sapphires – An update of the GRS research progress," 2018, http://gemresearch.ch/hpht-update), the ~3042 cm^{-1} series band is diagnostic of sapphire treated by a high-pressure, high-temperature process.

As shown in figure 39, the mineral inclusions melted and solidified within the surrounding discoid fractures, exhibiting a dendritic appearance. Micro-Raman spectra analysis on the white mineral and recrystallized dendritic

Figure 37. Blurred blue color zoning and melted white solid mineral inclusions surrounded by discoid fractures. Photomicrograph by Yujie Gao; field of view 5.26 mm.

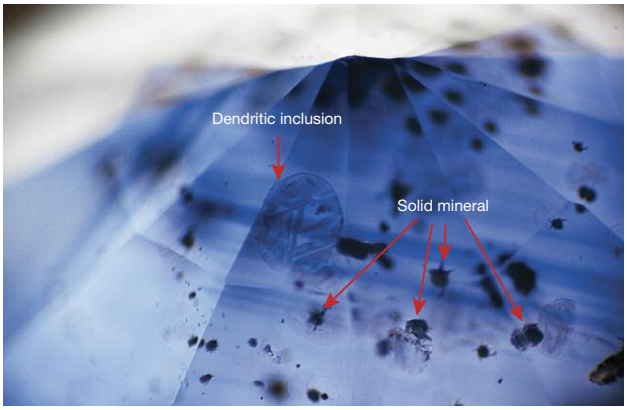

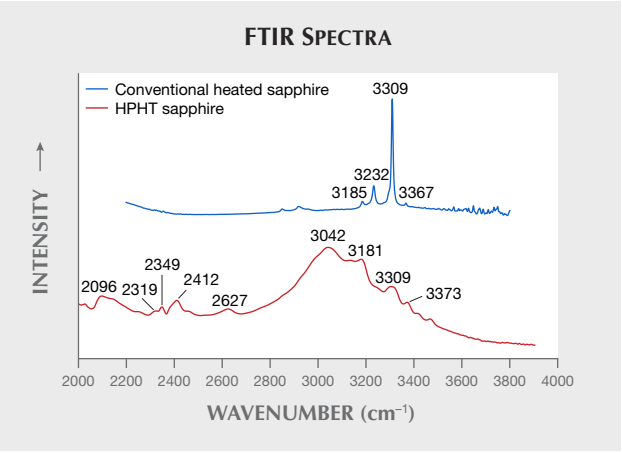

Figure 38. FTIR spectra of conventionally heated sapphire and the HPHT sapphire in figure 36. The latter showed distinct bands centered around 3042 cm^{-1}, accompanied by peaks at 2627, 2412, 2349, 2319, and 2096 cm^{-1}.

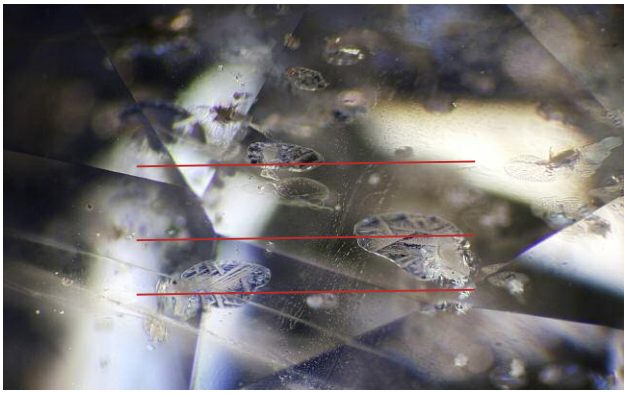

Figure 39. Discoid fractures were oriented in almost the same direction within the sapphire host. Photomicrograph by Yujie Gao; field of view 2.28 mm.

inclusions using 473 nm laser excitation produced some interesting results. The white melted minerals and the recrystallized inclusion showed almost the same peaks in the region of 1000–100 cm^{-1}, suggesting that they were the same mineral. Peaks at 641, 560, 541, 475, 334, and 221 cm^{-1} and a characteristic doublet at 188/178 cm^{-1} matched with the Raman spectrum for baddeleyite (a rare zirconium oxide mineral), according to the RRUFF database, as shown in figure 40.

Zircon ($ZrSiO_4$) is known as a common inclusion in sapphires, which may undergo solid state thermal dissociation to zirconia and silica at extreme conditions such as high temperature and/or high pressure as follows:

$$ZrSiO_4 \text{ (zircon)} \rightarrow ZrO_2 \text{ (baddeleyite)} + SiO_2$$

Baddeleyite, a monoclinic polymorph of zirconia, forms at relatively high pressure (up to about 7 GPa). W. Wang et al. ("The effects of heat treatment on zircon inclusions in Madagascar sapphires," Summer 2006 *G&G*, pp. 134–150)

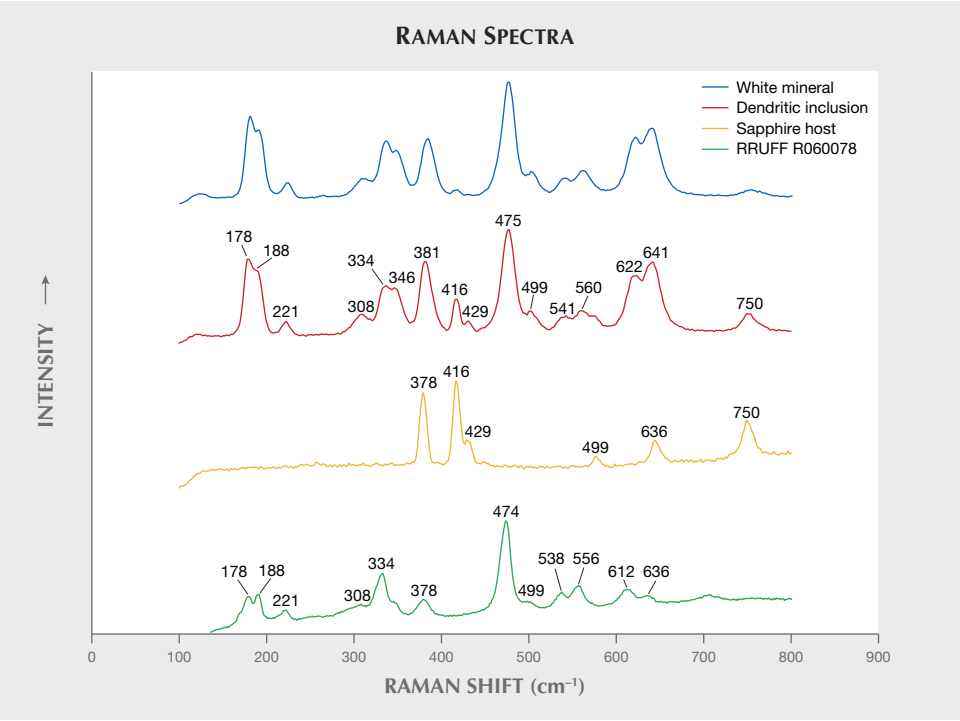

Figure 40. Raman spectra of the white mineral and dendritic inclusion both matched with baddeleyite (ZrO_2).

confirmed the existence of baddeleyite with zircon in heated blue sapphire by detecting a 188/178 cm^{-1} Raman doublet of baddeleyite in melted zircon after heating at around 1400–1700°C and normal pressure. The results of Wang et al. (2006) suggest that when using conventional heating techniques, only a small fraction of zircon transforms into baddeleyite, while most of the zircon inclusions keep their crystalline structure intact without any phase transformation. Based on our Raman testing, however, no zircon was found in this 7.11 ct sapphire, and spectra of both the white mineral at the center and the recrystallized minerals in the fracture were consistent with baddeleyite.

Additionally, we also noticed several fractures filled with baddeleyite in a uniform orientation (again, see figure 39). Using a polariscope and a conoscope under a microscope, we confirmed that these fractures occurred along the basal plane (0001) of the sapphire.

One question is whether these flat fractures already existed from parting before treatment (which is commonly encountered in sapphire) or formed during treatment. It is known that parting may occur along the basal plane of sapphire under certain situations, such as twinning or exsolution of inclusions. Neither distinct twinning nor exsolved inclusions were found, and almost all of the fractures were fully filled, leaving no empty space within them. Thus, we believe that these fractures could have been triggered by treatment. The proposed occurrence and healing process of these fractures are illustrated in figure 41.

In conclusion, we can appropriately speculate that PHT ("HPHT") treatment might cause flat fractures along the basal plane and facilitate the transformation from zircon to baddeleyite. The high baddeleyite content in heated sapphire may serve as a good indicator of PHT ("HPHT") treatment. Further experiments are needed to support this argument.

Xueying Sun and Yujie Gao
(peter.gao@guildgemlab.com)
Guild Gem Laboratories, Shenzhen, China

CONFERENCE REPORTS

2019 GSA annual meeting. The Geological Society of America (GSA) annual meeting took place in Phoenix, Arizona, September 22–25. GIA participated in the exhibition and hosted speaker and poster sessions that attracted great attention on gemology among the geoscience community (figure 42).

The talks started with research by **Dr. Tingting Gu** (formerly with GIA) on lower-mantle inclusions trapped in a type IaB diamond. The study identified inclusions of hydrous ringwoodite, ferropericlase, and enstatite (a back-transformation product of bridgmanite). This was the first evidence of them occurring together at this depth of the earth, which will help to unravel the pyrolytic nature of the 660 km discontinuity. The study was presented by co-author **Dr. Wuyi Wang** (GIA). **Dr. Sally Eaton-Magaña** (GIA) presented a detailed study of natural radiation stains in diamonds. Temperature-controlled experiments revealed that the stains' color changes from green to olive

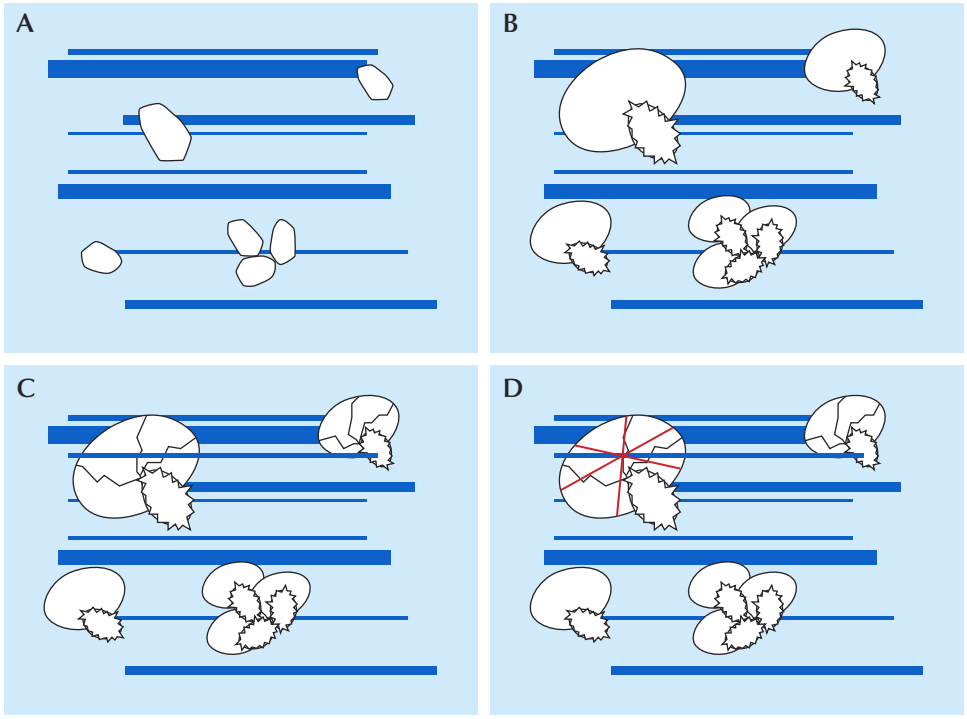

Figure 41. The occurrence and healing process of discoid fractures in the sapphire during treatment. A: Zircon inclusions and blue color bands in the sapphire. B: Under high pressure and high temperature, progressive decomposition of zircon results in the formation of baddeleyite and flat fractures. C: Baddeleyite penetrates into the discoid and fills the fracture with no space left. D: Baddeleyite recrystallizes in a dendritic pattern shown by the red line. Illustrations by Xueying Sun.

Figure 42. Presenters and session hosts from the gemology session at the 2019 GSA annual meeting. Front row, left to right: Sarah Steele, Dr. Christopher M. Breeding, Kyaw Soe Moe, and Rachelle Turnier. Back row: Dr. Evan Smith, William Aertker, Dr. Aaron Palke, Dr. Sally Eaton-Magaña, Roy Bassoo, Dr. Wuyi Wang, Samuel Martin, Dr. Jim Shigley, and Dr. John Valley. Photo by Tao Hsu.

green at about 400°C and then to brown at about 550–600°C. Color-changing rates of different related defects were then carefully calculated. This study provides needed information about the reliability of using radiation stain color to identify diamond color as either natural or treated. Graduate student **Roy Bassoo** (Baylor University) put forward a source study of Guyana diamonds mined from alluvial gravels in the Amazon rainforest. Several possible primary diamond sources were proposed, and multiple advanced analytical methods were used on rough diamond crystals. Detrital zircon dating ruled out West Africa as a potential source. Inclusion and isotopic data suggest that these diamonds are of upper-mantle peridotite paragenesis, with a subpopulation of eclogite paragenesis and an undiscovered kimberlite source that still needs to be identified. **Dr. Evan Smith** (GIA) shared the characteristics of the newly discovered nickel sulfide mineral crowningshieldite (α-NiS). This mineral was found as inclusions in a so-called CLIPPIR diamond (Cullinan-like, Large, Inclusion-Poor, Pure, Irregular, and Resorbed) that came from 350–750 km below the earth's surface. Crowningshieldite features one Ni atom connected to six sulfur atoms, while the known β-NiS features one connecting to five.

Dr. Christopher M. Breeding (GIA) discussed the rarity and color causes of orange diamonds. Orange diamonds account for only 2.4% of all colored diamonds, based on GIA's intake database. Single substitutional nitrogen and the 480 nm band are the two major mechanisms responsible for this rare color. Of the two, the 480 nm absorption band is not well understood and has been proposed to be composed of substitutional oxygen atoms in the diamond lattice. At low concentration this defect causes yellow color, while at high concentration the color shifts to orange. Diamonds with this defect can also be heated to temporarily change their color to orange. **Kyaw Soe Moe** (GIA) continued the discussion on the 480 nm band using the study results of a bicolor diamond. The 480 nm band was detected only in the brown-orange portion of this diamond. An interesting find was that the fluorescence image and optical image of this color zone do not match, which indicates that the 480 nm band caused color zoning that does not align with growth zones. This observation suggests that the defect causing the 480 nm absorption formed or penetrated the diamond after its growth. The authors proposed that the defect consists of localized vacancy clusters, in addition to other previously proposed possibilities.

Following a series of diamond presentations, the talks continued with colored gemstone discussions. Graduate student **Samuel Martin** (Brigham Young University) presented a geochemical comparison study of sapphires from Bingham Canyon in Utah and from Yogo Gulch, Montana.

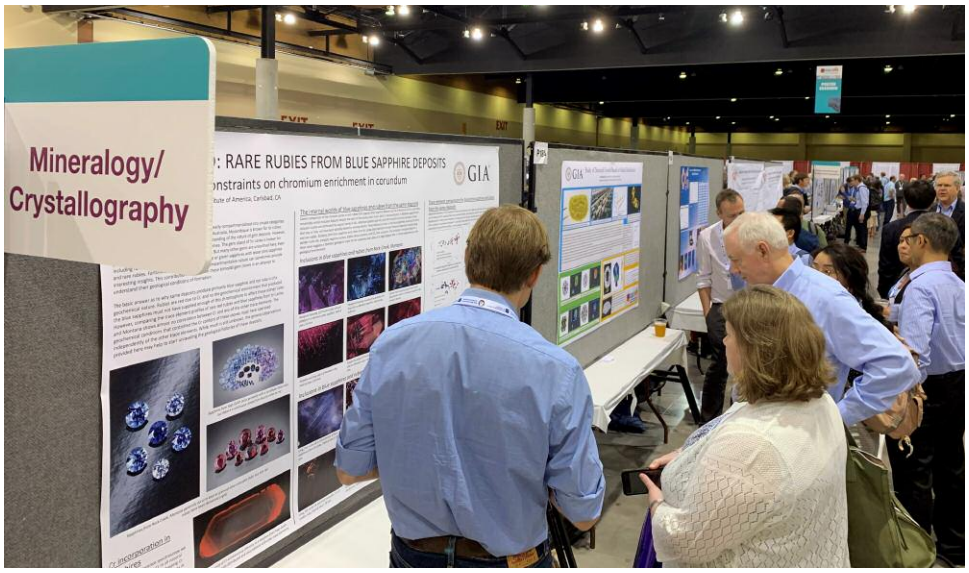

Figure 43. GSA poster presenters shared their latest research. Photo by Tao Hsu.

Although the two sapphire populations were formed 10 million years apart, they do broadly share the same trace element signatures, and both contain silica melt inclusions. Oxygen isotope study of both suggests that they have different protoliths, with Bingham Canyon sapphires as a mixture of multiple populations in the Bingham magma system. The study proposed that sapphires from both sources have been produced through partial melting of Al-rich rocks. Graduate student **Rachelle Turnier** (University of Wisconsin–Madison) shared her research on the genesis of basalt-related gem corundum with zircon inclusions in samples from nine different sources around the globe. Through a combination of element mapping, growth texture imaging, zircon geochronology, apparent pressure estimation, oxygen isotope study, and *in situ* geochemical analyses, variations were revealed among these deposits, which have generally been grouped in a single category. PhD candidate **William Aertker** (Colorado School of Mines) discussed the genesis of metasomatic sapphire from the Whitehorn stock metamorphic aureole in central Colorado. Sapphires occur within a ductile shear zone that experienced contact metamorphism. Extensive evidence suggests that desilication was not the only process involved in corundum formation. Element exchange must have happened at the same time, and ductile shearing facilitated fluid channeling to facilitate this exchange process, known as metasomatism. Retired geologist **Charles Breitsprecher** (California State University, Sacramento) presented a self-funded field investigation of sunstone from three mines in southeast Oregon. The occurrence and regional geology were discussed. Gemologist and professional lapidary **Sarah Steele** talked about her archaeogemological and chemistry study on gem-quality jet, including its use since the Upper Paleolithic and the market for it today. The author's analyses found 33 different hydrocarbons and biopolymers that are used as gems, which goes beyond the current commonly used definition for jet**. Dr. Aaron Palke** (GIA) closed the session with a presentation on the newly recognized mineral johnkoivulaite ($Cs[Be_2B]Mg_2Si_6O_{18}$), named in honor of renowned GIA researcher John Koivula. This new member of the beryl group was discovered in Mogok, an area full of opportunities to expand the mineral family. Due to its special structure, johnkoivulaite does not contain as much water as other members of the beryl group.

This year's poster session featured five presenters (figure 43). **Dr. Qishen Zhou** (China University of Geosciences, Wuhan) presented two posters, on the results of colored diamond and sapphire auctions, respectively. Dr. Zhou and his team collected more than 50,000 auction results over the past decade. These results are representative of the global auction sector, including the Chinese domestic auction sector, which is not well known to the rest of the industry. The colored diamond study poster focused on pink and blue diamonds. Both studies explored the relationship between auction results and the quality factors of the stones. The authors found that color largely determines colored diamonds' auction prices, while both color and carat weight have a high impact on sapphire. **Dr. Aaron Palke** (GIA) delivered research on rare rubies found in blue sapphire–dominant deposits. The study compared sapphires and rarely encountered rubies from four different sources. Geochemical results indicate that the trace element Cr, which causes the red color, behaves quite independently of the other trace elements. However, trace elements other than Cr share similarity between sapphires and rubies from the same deposit, which was also supported by inclusion scenes. **Paul Johnson** (GIA) displayed an interesting research project on melee-size HPHT lab-grown diamonds, which have a different crystal shape from large crystals made with the same method. The authors used element mapping of nickel to reveal the growth structure of these small diamonds. The results indicated multiple growth stages of the small lab-grown diamonds, which

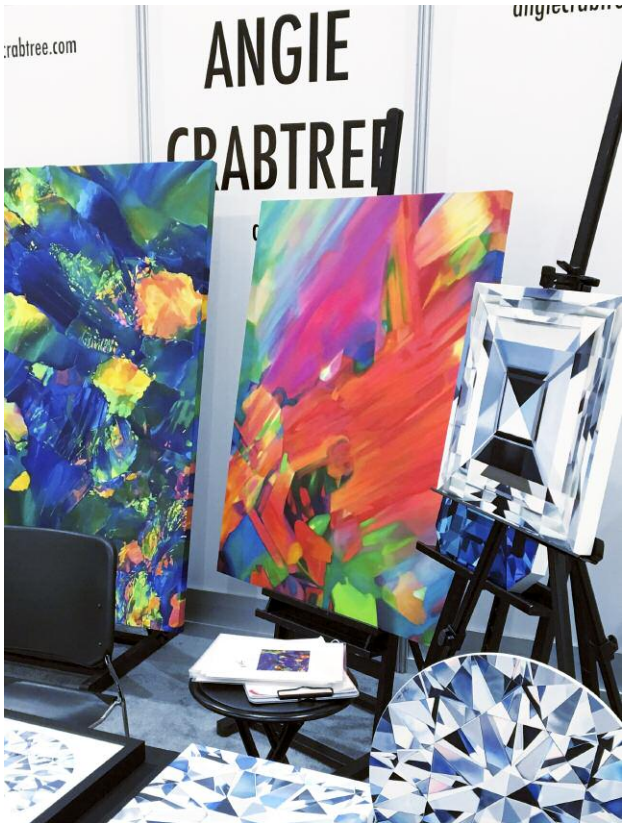

Figure 44. This selection of Angie Crabtree's paintings displayed at the AGTA GemFair showcases opal and cut diamond. Photo by GIA.

explained their elongated crystal shape. **Garrett McElhenny** (GIA) presented a study on type IIa pink diamonds. The author studied a suite of 30 samples with inclusions using Raman spectroscopy. The inclusions identified were mainly of sublithospheric origin. The existence of sublithospheric inclusions again proved that these diamonds came from the sublithospheric mantle.

The 2020 GSA annual meeting is scheduled for October 25–28 in Montreal.

Tao Hsu
GIA, Carlsbad

MISCELLANEOUS

Gemstone portrait artist Angie Crabtree. The 2019 AGTA show in Tucson featured the work of a gemstone portrait artist. On display in Angie Crabtree's booth were her oil paintings (figure 44) on canvas and panel. She also had a table with paints, palettes, and other supplies so people could see her at work (figure 45).

Crabtree's portraits range in size up to 64 × 48 inches. She said people are excited to see gemstones in great size and detail. One painting can take more than 300 hours to complete. She said because people outside the gem and jewelry industry don't always recognize the subjects as gemstones, the paintings can also be interpreted as abstract art.

The San Francisco–based artist said that all of her business, even from large corporate clients, comes from Instagram. "I've never paid to promote," Crabtree said. "I'm just very fortunate for that." Instagram also allows her to sell her own work instead of relying on galleries, which take a sizeable cut (typically around 50%). "That's hard for artists," she said. "Because of social media, artists have the opportunity to promote and market themselves."

Crabtree grew up on a ranch in Sonoma County, California, and was interested in nature and geology from a young age. Her grandfather used to go gold mining, and she would collect obsidian and other rocks along the way. She began painting and taking art classes at the age of five, and by 12 she was teaching painting. She attended an arts high school and college, studied abroad at Amsterdam's Gerrit Rietveld Academie, and graduated from the San Francisco Art Institute in 2009.

In 2012, while working as a high school art teacher, she did her first gemstone painting—a diamond portrait for an art gallery. She began painting different diamond cuts and posted them to Instagram. Soon people were asking for portraits of their engagement rings and other special stones. "That's when it really took off," she said.

Figure 45. Angie Crabtree at work at the AGTA show. Photo by Erin Hogarth.

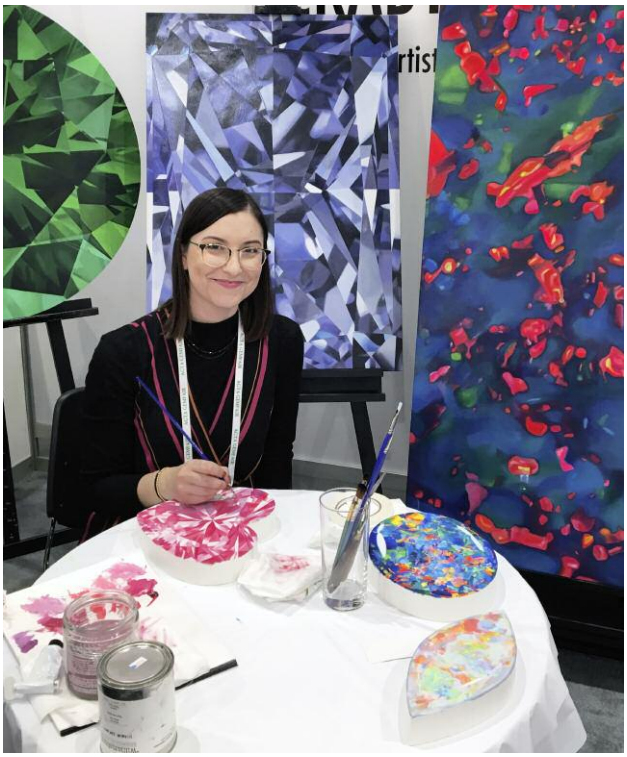

Figure 46. This 1.16 ct crystal of the new mineral johnkoivulaite was reportedly discovered in the legendary Mogok Valley of Myanmar in the Pein Pyit mining area. Photo by Robert Weldon/GIA.

One of the first people she met in the industry—via Instagram—was gemstone cutter Jean-Noel Soni of Top Notch Faceting. He told her about the gem industry and "completely opened my eyes," she said. "That's when I just fell in love with the whole thing."

In 2015, she established her business and quit her teaching job. "It was a pretty big leap," she said. "It's scary for any artist to do that." Within the first year, she was commissioned by Chopard and Forevermark to paint large series. Since then, business has grown to the point that she now has a studio manager who handles sales, accounting, and communication.

In 2018, Crabtree painted her first colored stone: an opal. "I wanted something a little bit more expressive and organic," she said. Then came a tsavorite and an alexandrite, and she has since moved into sapphires and other stones. She plans to eventually paint minerals and other natural objects.

Crabtree was trained in realism, but she said her biggest struggle has been understanding gemstone proportions and facet dimensions. She has consulted industry experts to learn how to use the correct dimensions and ratios for the stones in her paintings. She often does not see the actual stones—most clients send her photographs. Painting accurate colors can be challenging, she said, because of the way a gemstone's color changes with movement and light. Mixing color palettes is a laborious process: She will mix 30 or so colors and write down each color recipe for future use. "People think being an artist is painting all day every day, and it's not," she said. "It's numbers and talking to people, and it's sales and it's promotion. Even the cleanup and setup takes forever."

Crabtree has two autoimmune diseases. "There are certain days where I wake up and my hands are just stuck in fists. Sometimes I can't walk. Sometimes I can't open my paint," she said. "But I do what I love, and I get to create my own hours, and I get to travel. So I make it work and stay positive."

Erin Hogarth
GIA, Carlsbad

ANNOUNCEMENTS

Johnkoivulaite: A new gem mineral. A new mineral, johnkoivulaite, has been named in honor of John Koivula, a renowned microscopist and preeminent researcher at GIA for more than 40 years. In collaboration with scientists from the California Institute of Technology, Dr. Kyaw Thu of Macle Gem Trade Laboratory, and Nay Myo, a gem dealer from Mogok, GIA researchers described johnkoivulaite, which the International Mineralogical Association (IMA) formally accepted as a new mineral species on September 6, 2019.

The world's first specimen of johnkoivulaite was reportedly uncovered from the Pein Pyit mining area of Mogok in Myanmar. It subsequently passed through the hands of Nay Myo, a local gem dealer. When the 1.16 ct stone (figure 46) could not be identified, Nay Myo suspected he had encountered a new mineral and had the sample sent to GIA for identification. When the researchers

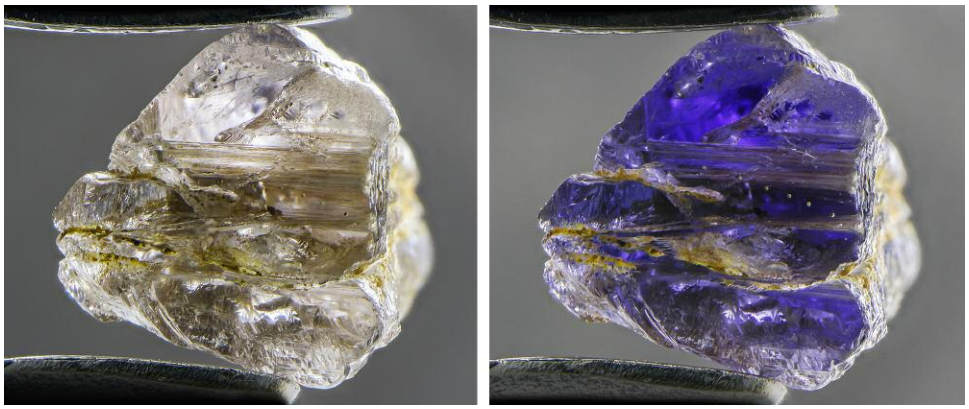

Figure 47. Johnkoivulaite shows strong pleochroism, going from near-colorless (left) to violet (right) when examined with polarized light. Photomicrographs by Nathan Renfro; field of view 10.05 mm.

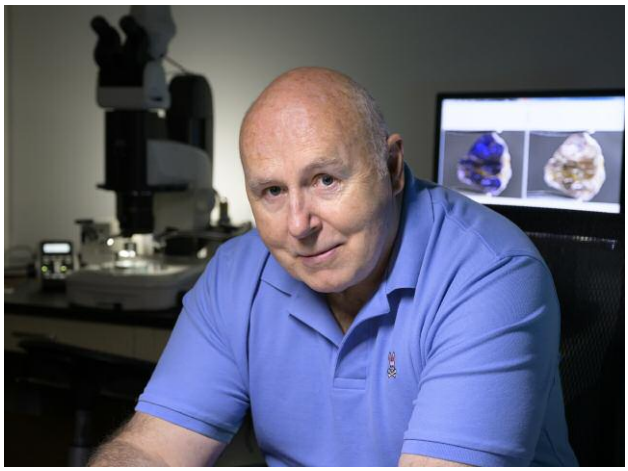

Figure 48. The new mineral johnkoivulaite is named after renowned gemologist John Koivula, best known for his contributions to inclusion research and photomicrography. Photo by Kevin Schumacher.

first examined the sample and realized its unique gemological properties, GIA made arrangements to purchase the unusual stone from Nay Myo so that additional advanced testing could be performed and the sample could be deposited in the GIA museum. Once the type specimen was housed in the museum (one of IMA's requirements for describing a new mineral), the team was able to submit a new mineral proposal. According to IMA guidelines, a new mineral can be named in recognition of a person's significant scientific contributions to the field of mineralogy. This one was named in honor of John Koivula's lifelong efforts to advance the sciences of mineralogy and gemology.

Single-crystal X-ray diffraction (XRD) analysis was performed in collaboration with researchers at the California Institute of Technology and indicated a hexagonal crystal structure that was very similar to beryl and other members of the beryl group such as pezzottaite. Chemical analysis by LA-ICP-MS and EPMA identified enrichment in cesium, boron, and magnesium and confirmed johnkoivulaite's membership in the beryl family, with its ideal end-member formula as $Cs(Be_2B)Mg_2Si_6O_{18}$. Standard gemological testing gave a refractive index of 1.608, with a birefringence too low to accurately measure, a specific gravity of 3.01, a hardness of 7 ½, a conchoidal fracture, vitreous luster, and no reaction to long-wave or short-wave UV. Especially notable is johnkoivulaite's strong pleochroism from deep violet to nearly colorless when observed with polarized light (figure 47).

John I. Koivula (figure 48) developed an interest in minerals and particularly their inclusions during childhood, when he found a quartz crystal with pyrite inclusions in North Bend, Washington. From there, Koivula earned degrees in geology and chemistry before working as an exploration geologist. In the 1970s, his career changed direction when a friend suggested the Graduate Gemologist program at GIA. He joined GIA in 1976 and began publishing gemological articles and short notes while refining his photomicrography techniques. In 1986, he co-authored with Edward J. Gübelin the immensely popular *Photoatlas of Inclusions in Gemstones*, which was followed by two additional volumes. Koivula also wrote *The Microworld of Diamonds* and co-authored *Geologica* with Robert Coenraads. Other highlights of his career include winning first place in Nikon's Small World Photomicrography competition in 1984, receiving the AGS's Robert M. Shipley Award in 1996, and being named one of *JCK* magazine's 64 Most Influential People in the Jewelry Industry in the 20th Century. In 2002, he was awarded the AGA's Antonio C. Bonanno Award for Excellence in Gemology. Mr. Koivula also received GIA's Richard T. Liddicoat Award for Distinguished Achievement in 2009 for his contributions to gemology.

After more than 40 years in the industry, Mr. Koivula still regularly contributes to gem and mineral research and is now a contributing editor for *G&G*'s Micro-World column.

The discovery of a new mineral is a rare and exciting occasion for the gemological community. It is a special honor for the authors to be able to name this mineral after such a prominent and well-deserving gemologist.

Aaron C. Palke, Ziyin Sun, and Nathan Renfro
GIA, Carlsbad

Lawrence M. Henling, Chi Ma, and George R. Rossman
California Institute of Technology, Pasadena

Kyaw Thu
Macle Gem Trade Laboratory, Yangon

Nay Myo
Greatland Gems and Jewelry, Mogok

Patcharee Wongrawang and Vararut Weeramonkhonlert
GIA, Bangkok

ERRATA

1. In the Spring 2019 GNI entry "Gray spinel: A new trend in colored stones" (p. 130), the figure 15 caption listed the incorrect carat weight and cutter. The gray spinel weighed 24.15 ct and was courtesy of 3090 Gems, LLC. We thank Bryan Lichtenstein for correcting this.

2. In the Summer 2019 article "A decade of ruby from Mozambique: A review" (pp. 162–183), the FTIR spectrum in figure 21D mislabeled the 3240 and 3161 cm^{-1} peaks. Also, the 2420 cm^{-1} peak should be disregarded, as it was caused by a fingerprint.